

Stretching of Proteins in the Entropic Limit

Marek Cieplak^{1,2}, Trinh Xuan Hoang³, and Mark O. Robbins¹

¹ *Department of Physics and Astronomy, The Johns Hopkins University, Baltimore, MD 21218*

² *Institute of Physics, Polish Academy of Sciences, Al. Lotników 32/46, 02-668 Warsaw, Poland*

³ *The Abdus Salam International Center for Theoretical Physics, Strada Costiera 11, 34014 Trieste, Italy*

(Dated: October 27, 2018)

Mechanical stretching of six proteins is studied through molecular dynamics simulations. The model is Go-like, with Lennard-Jones interactions at native contacts. Low temperature unfolding scenarios are remarkably complex and sensitive to small structural changes. Thermal fluctuations reduce the peak forces and the number of metastable states during unfolding. The unfolding pathways also simplify as temperature rises. In the entropic limit, all proteins show a monotonic decrease of the extension where bonds rupture with their separation along the backbone (contact order).

PACS numbers: 87.15.La, 87.15.He, 87.15.Aa

There is considerable current interest in the mechanical manipulation of single biological molecules. In particular, stretching studies of large proteins with atomic force microscopes (AFM) and optical tweezers [1, 2] reveal intricate, specific, and reproducible force (F) – displacement (d) curves that call for understanding and theoretical interpretation. The patterns depend on the pulling speed and on the stiffness of the pulling device [3]. They must also depend on the effective temperature given by the ratio of thermal to binding energies. In experiments this ratio can be varied slightly by changing temperature T , and over a large range by changing solvent properties [2], such as pH. While the role of effective temperature in folding is well studied [4, 5], its effect on mechanical unfolding is not.

In this paper, we report results of molecular dynamics simulations of simplified models of six proteins that reveal universal trends with increases in the effective temperature. Thermal fluctuations accelerate rupture, lower the peaks in the $F - d$ curves, and reduce the number of peaks. Most interestingly, the succession of unfolding events simplifies from a complex pattern determined by the energy landscape into a simple, uniform pattern determined by entropic considerations. All of these changes are gradual, and move to completion near the T where the specific heat peaks. In the entropic limit, rupturing events are governed exclusively by the contact order, i.e. by the distance along a sequence between two amino acids which make a contact in the native state. The contact order is also believed to be the major influence in folding to the native state. However, there is no general correlation between folding and the extremely complex unfolding scenarios observed at low T [3].

The models we use are coarse-grained and Go-like [6]. Full details are provided in earlier studies of folding [5, 7]. Briefly, the amino acids are represented by point particles of mass m located at the positions of the C^α atoms. They are tethered by a strong harmonic potential with a minimum at the peptide bond length. The native structure of a protein is taken from the PDB [8] data bank and the interactions between the amino acids are divided into native and non-native contacts. The distinction is made by

taking the fully atomic representation of the amino acids in the native state and then associating native contacts with overlapping amino acids. The criterion for overlaps uses the van der Waals radii of the atoms multiplied by 1.24 to account for the softness of the potential [9].

The interaction between each pair of overlapping acids i and j is described with a 6-12 Lennard-Jones (LJ) potential whose interaction length σ_{ij} (4.4 – 12.8 Å) is chosen so that the potential energy minimum coincides with the native $C^\alpha - C^\alpha$ distance. This forces the ground state to coincide with the native state at room T . The non-native contacts are described by a LJ potential with $\sigma = 5\text{Å}$ that is truncated at $r > 2^{1/6}\sigma$ to produce a purely repulsive force. An energy penalty is added to states with the wrong chirality as described in Ref. [5]. This facilitates folding, but has little effect on mechanical stretching since the protein starts with the correct chirality. All of the potentials have a common energy scale ϵ , which is taken as the unit of energy. Time is measured in terms of the usual LJ vibrational time scale $\tau \equiv \sqrt{m\sigma^2/\epsilon}$.

The desired effective temperature $\tilde{T} \equiv k_B T/\epsilon$, where k_B is Boltzmann's constant, is maintained by coupling each C^α to a Langevin noise [10] and damping constant γ . The value of $\gamma = 2m/\tau$ is large enough to produce the overdamped dynamics appropriate for proteins in a solvent [5], but about 25 times smaller than the realistic damping from water. Previous studies show that this speeds the dynamics by about a factor 25 without altering behavior, and tests with larger γ confirmed that it merely rescales the diffusion time in the overdamped regime [7]. As a result the effective value of τ in simulations is about 75 ps.

Stretching is accomplished by attaching both ends of the protein to harmonic springs of spring constant $k = 0.12\epsilon/\text{Å}^2$ [3]. This corresponds to a cantilever stiffness $k/2 \sim 0.2\text{N/m}$, which is typical of an AFM. Stretching is implemented parallel to the initial end-to-end position vector of the protein. The outer end of one spring is held fixed at the origin, and the outer end of the other is pulled at constant speed $v_p = 0.005 \text{Å}/\tau$. Previous studies at $\tilde{T} = 0$ showed that decreasing the velocity below

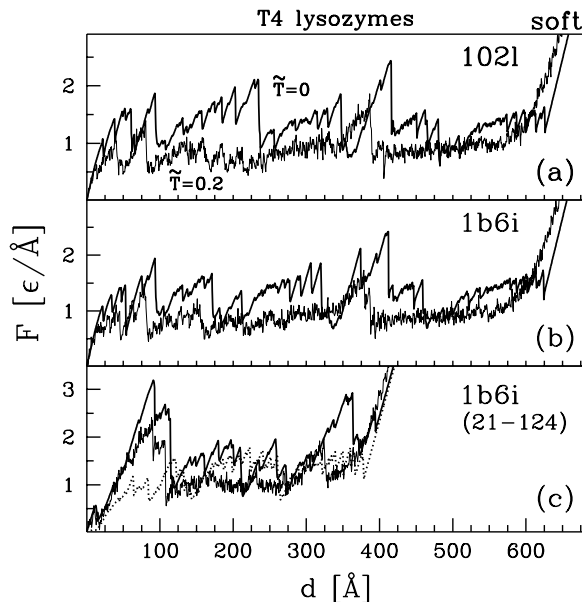


FIG. 1: $F-d$ curves for three lysozyme systems: (a) 1021, (b) 1b6i pulled from its ends and (c) 1b6i pulled by the cysteins at locations 21 and 124. Thick and thin solid lines correspond to $\tilde{T}=0$ and 0.2, respectively. The dashed line in (c) shows $\tilde{T}=0$ results for 1b6i with the 1-20 and 125-163 amino acids removed.

this value had little effect on unfolding [3]. This velocity corresponds to about 7×10^6 nm/s. Velocities in all atom simulations are more than three orders of magnitude faster [14], but experimental AFM velocities are 1000 times slower. Closing this gap remains a formidable challenge. Varying the simulation temperature is one way to accelerate experimental dynamics into an accessible range.

The displacement of the pulled end of the spring is denoted by d . The net force stretching the protein is denoted by F , and measured from the extension of the pulling spring. Except at $\tilde{T}=0$, where the results are strictly reproducible, F is averaged over a displacement of 0.5 \AA to reduce thermal noise without substantially affecting spatial resolution. A contact between amino acids i and j is considered ruptured if the distance between them exceeds $1.5 \sigma_{ij}$. The unfolding scenario is specified by the unbinding or breaking distance d_u for each native contact. Note that at finite \tilde{T} the contact may break and reform several times and d_u is associated with the final rupture.

To illustrate the sensitivity of low \tilde{T} unfolding to small structural changes, we consider bacteriophage T4 lysozymes. There are two mutant structures with sequence length $N=163$ whose PDB codes are 1021 and 1b6i. The latter has cysteins in locations 21 and 124 instead of threonine and lysine respectively. Although the root mean square deviation between the two structures is merely 0.3 \AA , there are noticeable differences in the $\tilde{T}=0$ simulations of stretching in Fig. 1 (thick lines). The force

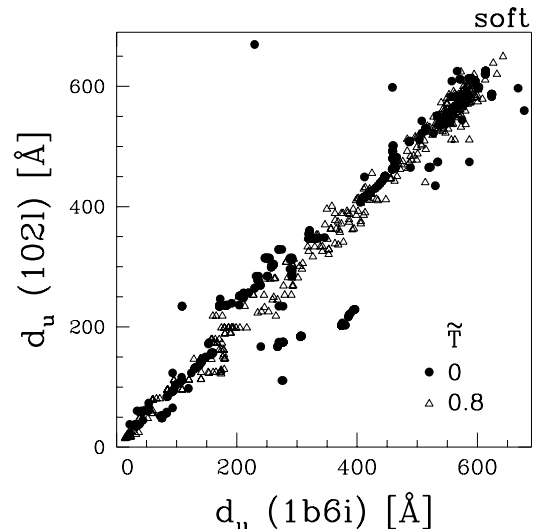


FIG. 2: Breaking distances for bonds in 1021 plotted against corresponding values for 1b6i at the indicated \tilde{T} .

curves show a series of upward ramps where the protein is stuck in a metastable state [3], followed by sharp drops as one or more contacts break, allowing the intervening segment to stretch. The differences between results for the two lysozymes, especially around d of 200, 375, and 475 \AA , indicate different sets of broken contacts. Fig. 2 compares the rupturing distances of each native contact in the two mutants. If the mutants followed the same pattern, the points would lie on a line with unit slope. However, they clearly follow different patterns at $\tilde{T}=0$. Sensitivity of $F-d$ curves to point mutations has been demonstrated in recent experiments on an immunoglobulin module in human cardiac titin [11].

Figure 1 (c) shows the importance of the location of the pulling force. Here the pulling springs were attached to the cysteins at $i=21$ and 124 of 1b6i, shortening the effective sequence length to 104 amino acids. Yang et al. [2] have used an AFM to study a string of 1b6i proteins bound covalently at these sites, and observe a series of equally spaced peaks that indicates the repeated units unfold sequentially. As shown in our earlier work [3], sequential unfolding occurs when the largest force peak breaks the first contacts in a repeat unit. Pulling from the $i=21$ and 124 sites produces a strong peak near the start of unfolding, which is consistent with the sequential unfolding observed by Yang et al.. This peak is absent for the full lysozymes and for the sequence from $i=21$ to 124 with amino acids $1-20$ and $125-163$ removed (dashed line). We would thus predict repeated arrays of the full or truncated sequences would unfold simultaneously if linked at their ends. It would be interesting to test these predictions with experiments. Note that recent experiments on another protein, E2lip3, have demonstrated that $F-d$ patterns can depend strongly on the pulling geometry, particularly the direction of the force relative

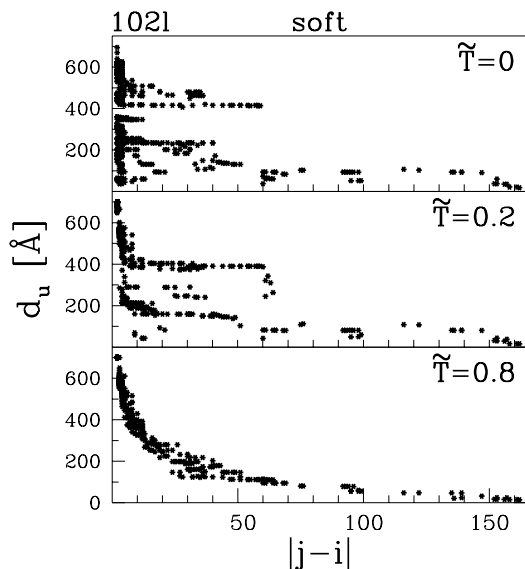


FIG. 3: Contact breaking distances for 102l vs. contact order at the indicated \tilde{T} .

to key native contacts [12].

We now turn to the effect of temperature on the force and unfolding sequence. Increasing \tilde{T} to 0.2 (thin lines in Fig. 1) produces similar changes in the force curves for all lysozymes. Thermal activation reduces the force needed to rupture bonds, shifting the entire force curve downwards. Some peaks disappear, indicating that the states are no longer metastable at this stress and \tilde{T} . Studies of the largest peaks show that they decrease roughly linearly with \tilde{T} , and shift to smaller d_u . For $\tilde{T} > 0.6$ no maxima can be identified and the curves approach the entropic limit of a worm-like-chain (WLC) [13] at higher \tilde{T} .

The force curves and unfolding scenarios (Fig. 2) of the two mutant structures become more similar with increasing \tilde{T} . Similar plots of the unfolding sequences for stiff vs. soft pulling springs also show considerable differences at low \tilde{T} that disappear as \tilde{T} rises. Fig. 3 shows that the sequence of unfolding distances also simplifies dramatically with increasing \tilde{T} . Values of d_u for each bond in 102l are plotted against the bond's contact order $|j-i|$. The $\tilde{T} = 0$ unravelling scenario is complex: Low contact order bonds break over the entire range of d_u , while middle and long-range bonds break in clusters of events at a few d_u . At $\tilde{T} = 0.2$, the events collapse onto a smaller set of lines. By $\tilde{T} = 0.8$, events have nearly collapsed onto a monotonically decreasing curve, that sharpens with further increases in \tilde{T} .

The simplification in unfolding sequence is even more dramatic for the tandem arrangement of three I27 domains of titin shown in Fig. 4. At $\tilde{T} = 0$, there is a serial unwinding of the individual domains that produces a repeated pattern. One domain unfolds from $d_u = 0$ to 300Å, the next from 300 to 600Å, and the last from 600 to 900Å. The three sequences can be overlapped by

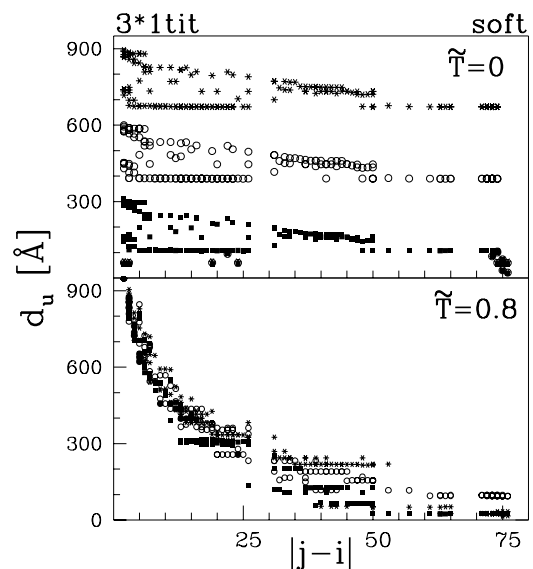


FIG. 4: Unravelling of three serial domains of titin on the $d_u - |j-i|$ plane. Squares (stars) correspond to the most forward (backward) domain.

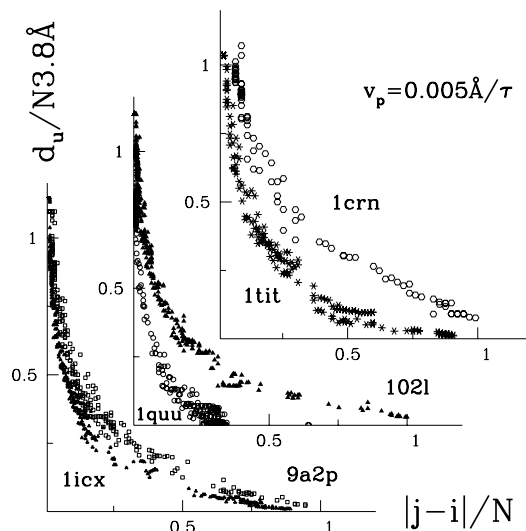


FIG. 5: Unfolding in the high \tilde{T} limit for 1crn (crambin; $N=46$), 1tit (the I27 domain of titin; $N=89$), 1iquu (actinin; $N=248$), 102l (lysozyme; $N=163$), 9a2p (barnase; $N=108$), and 1icx (yellow lupin protein 10; $N=155$). Both axes scaled by N and d_u is divided by the peptide bond length of 3.8Å to make it dimensionless. For each protein the value of \tilde{T} needed to reach the entropic limit was near \tilde{T}_{\max} . These values were 0.6, 0.8, 1.2, 1.4, 0.8, and 1.2 respectively.

a vertical displacement. By $\tilde{T} = 0.8$, unfolding occurs simultaneously and d_u has collapsed onto a nearly monotonic curve similar to that found in Fig. 3.

We have examined the \tilde{T} -dependence of unfolding for a large number of proteins, including periodically repeated domains. In all cases, increasing \tilde{T} produces a gradual

reduction in the size and number of force peaks and an increasingly universal relation between d_u and contact order. These changes saturate near the temperature \tilde{T}_{\max} where each protein has a maximum in the equilibrium specific heat. Fig. 5 compares the normalized unfolding curves for six proteins at temperatures near their \tilde{T}_{\max} . For each protein, d_u decreases nearly monotonically at this \tilde{T} . The curves are qualitatively similar, but results for shorter proteins tend to lie above those for longer proteins. Studies of the rate dependence show that this is because longer proteins take more time to sample configurations and thus are less likely to reform contacts with large $|j - i|/N$. The curves can be made more universal by choosing different pulling rates for each protein. Studies with artificial proteins (homopolymers), where every contact is native, indicate a logarithmic rate dependence with the normalized curves moving gradually up and to the right.

It is not surprising that \tilde{T}_{\max} is the temperature where unfolding simplifies. It is where the entropy of the system is changing most rapidly, and thus where binding energies are becoming less important. Not surprisingly, the thermal energy at \tilde{T}_{\max} is always comparable to the contact energy ϵ . Other characteristic temperatures for folding are substantially lower, and do not correlate well with the simplification of the unfolding sequence. For example, the temperature where folding is fastest, \tilde{T}_{\min} , is 0.35 for our model of 102l and the temperature where the protein spends half of its time in the unfolded state is 0.25. At both of these \tilde{T} 's the contact dependence of the

rupture process is still structured and non-monotonic, as illustrated in Fig. 3.

In summary, thermal fluctuations affect the force – displacement curves in a profound manner, reducing force peaks and the number of metastable configurations. Yang et al. [2] have observed the decrease in unbinding force with increasing \tilde{T} by modifying the solvent to reduce ϵ . However, as in our simulations for their tandem lysozyme system, domains unfold serially and there is little structure except for the initial force peak. Studies of systems that unfold serially would exhibit richer changes with \tilde{T} and we predict this should be observed for lysozymes joined at their ends.

Raising \tilde{T} produces a dramatic simplification of the unfolding sequence that culminates in a monotonic drop of d_u with contact order. In the entropic limit, $\tilde{T} > \tilde{T}_{\max}$, the tension in the chain is consistent with the WLC model [13]. However, this model is often used to describe unfolding at temperatures where folding is rapid. In this regime we find substantial deviations from the WLC model, which may affect the interpretation of experimental data. It would be desirable to repeat our studies with detailed atomistic potentials like those used for titin [14], but such studies remain too computationally intensive for a thorough scan of parameter space.

This work was supported by the Polish Ministry of Science (grant 2 P03B 032 25) and NSF Grant DMR-0083286. MC appreciates discussions with A. Sienkiewicz.

-
- [1] M. Rief, M. Gautel, F. Oesterhelt, J. M. Fernandez, and H. E. Gaub, *Science* **276**, 1109-1112 (1997); A. F. Oberhauser, P. E. Marszalek, H. P. Erickson, and J. M. Fernandez, *Nature* **393**, 181-185 (1998); M. Rief, J. Pascual, M. Saraste, and H. E. Gaub, *J. Mol. Biol.* **286**, 553-561 (1999); M. S. Z. Kellermayer, S. B. Smith, H. L. Granzier, C. Bustamante, *Science* **276**, 1112-1116 (1997); L. Tskhovrebova, K. Trinick, J. A. Sleep, M. Simmons, *Nature* **387**, 308-312 (1997); B. L. Smith, T. E. Schaeffer, M. Viani, J. B. Thompson, N. A. Frederic, J. Kindt, A. Belcher, G. D. Stucky, D. E. Morse, and P. K. Hansma, *Nature* **399**, 761-763 (1999).
- [2] G. Yang, C. Ceconi, W. A. Baase, I. R. Vetter, W. A. Breyer, J. A. Haack, B. W. Matthews, F. W. Dahlquist, and C. Bustamante, *Proc. Nat. Acad. Sci.* **97**, 139-144 (2000).
- [3] M. Cieplak, T. X. Hoang, and M. O. Robbins, *Prot. Struct. Func. Gen.* **49**, 104-113 (2002); 114-124 (2002).
- [4] N. D. Socci and J. N. Onuchic, *J. Chem. Phys.* **101**, 1519-1528 (1994)
- [5] M. Cieplak and T. X. Hoang. *Biophys. J.* **84**, 475-488 (2003).
- [6] H. Abe, N. Go, *Biopolymers* **20**, 1013-1031 (1981); S. Takada, *Proc. Natl. Acad. Sci. USA* **96**, 11698-11700 (1999); N. V. Dokholyan, S. V. Buldyrev, H. E. Stanley, and E. I. Shakhnovich, *Folding Des.* **3**, 577-587 (1998).
- [7] T. X. Hoang and M. Cieplak, *J. Chem. Phys.* **112**, 6851-6862 (2000); **113**, 8319-8328 (2001).
- [8] F. C. Bernstein, T. F. Koetzle, G. J. B. Williams, E. F. Meyer Jr., M. D. Brice, J. R. Rodgers, O. Kennard, T. Shimanouchi, and M. Tasumi, *J. Mol. Biol.* **112**, 535-542 (1977).
- [9] J. Tsai, R. Taylor, C. Chothia, and M. Gerstein, *J. Mol. Biol.* **290**, 253-266 (1999); G. Settanni, T. X. Hoang, C. Micheletti, and A. Maritan, *Biophys. J.* **83**, 3533-3541 (2002).
- [10] G. S. Grest, K. Kremer, *Phys. Rev. A* **33**, 3628-3631 (1986).
- [11] H. Li, M. Carrion-Vazquez, A. F. Oberhauser, P. E. Marszalek, and J. M. Fernandez, *Nature Struct. Biol.* **7**, 1117-1120 (2000).
- [12] D. J. Brockwell, E. Paci, R. C. Zinober, G. S. Beddard, P. D. Olmsted, D. A. Smith, R. N. Perham, and S. E. Radford, *Nature Struct. Biol.* **10**, 731 - 737 (2003).
- [13] M. Doi, and S. F. Edwards, *The Theory of Polymer Dynamics*, Oxford U.P., Oxford, England (1989).
- [14] H. Lu, B. Isralewitz, A. Krammer, V. Vogel, K. Schulten, *Biophys. J.* **75**, 662-671 (1998).